JOURNAL OF AIRCRAFT
Vol. 43, No. 1, January–February 2006

Multidisciplinary Design Optimization for Aeromechanics and Handling Qualities

Dario Fusato* and Roberto Celi†
University of Maryland, College Park, Maryland 20742

A design optimization study is presented in which rotor dynamics and flight dynamics are simultaneously taken into account to maximize the damping of a rotor lag mode. The design variables include rotor, airframe, and flight control system parameters. The constraints address rotor stability and loads and handling qualities. Two design optimization cases are considered, one with only constraints computed from the linearized model of the helicopter and the other with additional constraints that require the integration of the nonlinear equations of motion. Both finite difference and semi-analytical gradients are used for some constraints. The optimization procedure increases the lag mode damping by up to 90%, while satisfying all of the constraints, primarily by reducing the blade torsion stiffness. The aeromechanic design problem is a multidisciplinary problem. The constraint active at the optimum is the level 1 handling qualities requirement in the pitch axis. Optimization provides a framework to manage multidisciplinary problems systematically and efficiently. Using semi-analytical gradients of the constraints computed from the linearized model yields the same results as with finite difference gradients, but more efficiently. The computational advantage increases with problem size. Further advances in computer hardware and in optimization algorithms, including efficient sensitivity analyses, will help make numerical optimization a practical design tool.

Nomenclature

c	=	blade chord
D	=	distance from level 1 boundaries in ADS-33 charts[8]
F_{hub}	=	rms value of rotor hub forces and moments
$F(\boldsymbol{X})$	=	objective function
GJ	=	blade torsion stiffness
$g(\boldsymbol{X})$	=	constraint
K_θ, K_q	=	pitch attitude and rate feedback to longitudinal cyclic
K_ϕ, K_p	=	roll attitude and rate feedback to lateral cyclic
L, M, N	=	components of hub moment
p, q	=	roll and pitch rates of the helicopte
S_{HT}	=	area of horizontal tail surface
X, Y, Z	=	components of hub force
$\boldsymbol{X}$	=	vector of design variables
x_i	=	chordwise distance of blade c.g. from elastic axis
$\Delta\phi_{\min}$, $\Delta\theta_{\min}$	=	roll and pitch attitude changes in maneuver
ζ	=	damping ratio
τ_p	=	phase delay
ϕ_{pk}, θ_{pk}	=	peak roll and pitch rates in maneuver
ω_{BW}	=	bandwidth

Subscript

0	=	baseline design

Introduction

TECHNICAL advances, such as bearingless rotor systems and high-gain, mission-tailored flight control systems, can provide modern helicopters with unprecedented maneuverability, agility and increased mission effectiveness. At the same time, the design of these advanced helicopters has become more challenging because it requires the careful integration of several engineering disciplines. For example, advanced flight control systems can improve handling qualities, but may also reduce aeromechanic stability. A multidisciplinary approach to helicopter design clearly requires the analysis of the mutual interactions among a variety of design parameters. The analyses can be quite complex, and improved mathematical tools are desirable. Numerical optimization techniques can potentially be useful tools to tackle multidisciplinary helicopter design problems. A detailed discussion of the literature in the field is beyond the scope of the present paper. Information on the application of formal design optimization techniques to helicopter problems can be found in several surveys, such as Refs. 1 and 2 and Ref. 3, which also addresses some of the reasons why the acceptance of these techniques has been slower in the helicopter community than in other branches of engineering practice.

The problem of an optimal aeroelastic design of helicopter rotors for longitudinal handling qualities improvement was studied in Ref. 4. This paper describes an optimization study in which the torsional stiffness of a hingeless rotor blade and its cross-sectional offsets were optimized to stabilize the phugoid oscillation of the aircraft by increasing the stabilizing effect of the rotor. A sequence of approximate optimization problems was used to reduce the computational effort that otherwise would have been prohibitive. A very simple, linearized stability derivative-type model was used, and the rotor contribution to the derivatives was calculated from an isolated rotor analysis.

In Refs. 5–7, a multidisciplinary optimization of rotor and flight control system with aeroelastic stability and handling qualities constraints was performed. The handling qualities constraints enforced a subset of the ADS-33 handling qualities specifications.[8] The design variables were flap stiffness, flap–lag elastic coupling factor, and flight control system parameters. A technique for the calculation of gradients of constraints was developed. To reduce the computational cost, the gradients were calculated using low-order linear approximations, which were applied to the full linear model of the helicopter. The objective function to be reduced was a weighted average of the swashplate control displacements and rates for two preassigned maneuvers. The scheme adopted in Ref. 6 showed that lower control effort can be achieved if rotor and flight control system designs are performed simultaneously. The analysis was carried out for a coupled rotor–fuselage model with rigid blades.[9,10]

Extensive work in the area of flight control system optimization with ADS-33-based constraints has been performed by

Received 29 January 2004; accepted for publication 11 April 2004.

*Ph.D. Candidate, Department of Aerospace Engineering, Alfred Gessow Rotorcraft Center.

†Professor, Department of Aerospace Engineering, Alfred Gessow Rotorcraft Center.

Tischler et al.[11] and Colbourne et al.,[12] for example. The primary tool for this research is the CONDUIT computer code, which couples a sequential quadratic programming optimizer with an extensive set of ADS-33-based handling qualities constraints and a graphical user interface. The designer monitors the progress of the optimization, and can interact with the numerical optimizer to evaluate and adjust constraints and to explore tradeoffs. CONDUIT is generally used with linearized models of the helicopter, obtained from simulation or system identification of flight-test results, and the design variables are typically the parameters of the flight control system. In Ref. 12, CONDUIT was successfully used to perform a control law design and optimization for two helicopters, namely, the Kaman SH-2F Seasprite and the research helicopter RASCAL, based on the UH-60A Blackhawk.

In a recently completed study,[13] Fusato addressed the problem of the multidisciplinary optimization of a helicopter with rotor dynamic and handling qualities constraints. To reduce the computational costs, the gradients of the constraints computed from the linearized model of the helicopter were calculated using a new semi-analytical approach,[13–15] which proved far more efficient than using finite difference approximations. Very promising results were also obtained for the efficient calculation of those constraints that require the integration of the nonlinear equations of motion of the helicopter, to simulate the response to pilot inputs.[16] Finally, a complete optimization study was performed. The simulation included a fully coupled model of the flap–lag–torsion elastic motion of the blades, with no restriction on the magnitude of the hub motions.

The present paper is based on the research of Ref. 13 and has the following primary objectives:

1) Whether it is possible to increase the rotor lag mode damping by a proper design of rotor, airframe, and flight control system, while at the same time maintaining the stability of all the other rotor modes, and satisfying a representative subset of the ADS-33 handling qualities specification is studied.

2) Whether the aeromechanic design problem is multidisciplinary in nature, or whether rotor dynamics and handling qualities can be addressed independently is determined.

3) Approximate, but efficient, semi-analytical gradients of the constraints computed from the linearized model are applied to a full optimization procedure, and the impact on accuracy and computational efficiency is assessed.

Helicopter Simulation Model

The simulation model used in this study is a blade element-type, coupled rotor–fuselage model. The blades are modeled as flexible beams undergoing coupled flap–lag–torsion deformations.[17] The rotor equations of motion are discretized using finite elements, and a modal coordinate transformation is used to reduce the number of rotor degrees of freedom. The extended momentum theory of Keller[18] is used to model the main rotor inflow. A one-state dynamic inflow model is used for the tail rotor. Quasi-steady stall and compressibility effects are introduced through look-up tables of airfoil aerodynamic coefficients. No restrictions are placed on the magnitude of the hub motions: The aerodynamic and inertia effects of the kinematics of large-amplitude maneuvers are rigorously taken into account in the formulation of the rotor equations.

The rigid-body motion of the fuselage is described through nonlinear Euler equations. The aerodynamic characteristics of the fuselage and of the empennage are described by look-up tables of aerodynamic coefficients. The dynamic coupling between the rotor and the fuselage is rigorously modeled, whereas the aerodynamic coupling is neglected.

The trim procedure simulates free flight and simultaneously enforces overall force and moment equilibrium on the aircraft, as well as the periodicity of the steady-state motion of the rotor. The trim calculations for the results of this paper consisted of the solution of a set of 50 nonlinear algebraic equations. The linearized model used for the calculation of the poles and of the frequency responses was extracted numerically by perturbing the equations of motion of the helicopter at a number of equispaced azimuth locations, performing a multiblade coordinate transformation, and averaging the state and control matrices to eliminate the periodic terms. Because the coupled rotor–fuselage model consisted of 53 differential equations, the linearized system had size 53. The response to pilot inputs was computed by direct numerical integration of the equations of motion.

Table 1 Design variables and side constraints

Design variable	Lower bound	Baseline	Upper bound
$\Delta S_H/S_H$	−0.5	0	2
$\Delta GJ/GJ$	−0.5	0	2
$\Delta x_i/c$, %	−2	0	2
$\Delta c/c_0$	−0.2	0	0.8
K_θ, %/rad	0	0	300
K_q, %s/rad	0	0	300
K_ϕ, %/rad	0	0	300
K_p, %s/rad	0	0	300

Formulation of the Optimization Problems

The optimization problems are formulated in nonlinear mathematical programming form as follows. Find a vector $\boldsymbol{X}$ of design variables such that the objective function $F(\boldsymbol{X}) \rightarrow$ minimum, subject to behavior constraints $g_j(\boldsymbol{X}) \leq 0$, $j = 1, \ldots, m$, and side constraints $\boldsymbol{X}_L \leq \boldsymbol{X} \leq \boldsymbol{X}_U$ on the design variables, where the subscripts L and U denote lower and upper bounds, respectively.

Two optimizations will be carried out. In the first, the behavior constraints will be limited to those that can be evaluated using only the linearized model of the helicopter. The first optimization will be repeated twice, first using finite difference-based gradients of objective function and constraints and then using a more efficient semi-analytical method for both objective and constraints. The second optimization will also include constraints that require the integration of the nonlinear equations of motion, for which only finite difference-based gradients will be used. Objective function and side constraints are the same for both optimizations. The flight speed in both cases is 40 kn.

The purpose of the optimization is to maximize the damping ratio ζ of the least damped mode of the baseline configuration, which is the progressive lag mode. Therefore, the objective function $F(\boldsymbol{X})$ is defined as

$$F(\boldsymbol{X}) = -\zeta/\zeta_0 \rightarrow \min \tag{1}$$

where ζ_0 is the damping ratio of the initial design and is used here as a scaling factor to keep the value of $F(\boldsymbol{X})$ of the order of one. The design variables, and their respective upper and lower bounds, are presented in Table 1. The design variables are actually implemented in normalized form, and all vary between 0 (variable at its lower bound) and 1 (variable at its upper bound). The ith design variable X_i can be obtained from the normalized design variable α_i using

$$X_i = (1 - \alpha_i)X_{Li} + \alpha_i X_{Ui} \tag{2}$$

where X_{Li} and X_{Ui} are, respectively, the lower and upper bound for the design variable X_i.

Optimization Case 1

For this optimization, the behavior constraints are obtained exclusively from the state-space linearized model of the helicopter. The constraints obtained from the time integration of the nonlinear equations of motion are not included. The behavior constraints are divided in two groups, namely, handling qualities constraints and rotor dynamics constraints.

Handling Qualities Constraints

The first is level 1 bandwidth/phase delay in pitch. This constraint is implemented on the basis of the specification chart of Sec. 3.3.2.1 of ADS-33 (Ref. 8) for the target acquisition and tracking mission task element (MTE). The distance $D_{\text{pitch},s}$ of the point representative

of the helicopter from the level 1 boundary ($D_{\text{pitch},s}$ negative if the point is in the level 1 region) must be negative:

$$g(\boldsymbol{X}) = D_{\text{pitch},s} \leq 0 \tag{3}$$

The second constraint is level 1 bandwidth/phase delay in roll. Similarly,

$$g(\boldsymbol{X}) = D_{\text{roll},s} \leq 0 \tag{4}$$

where $D_{\text{roll},s}$ is the distance from the level 1 boundary in the roll specification chart.

The third constraint is compliance with mid-term response specification at least 25% better than baseline design. The constraint is implemented as

$$g(\boldsymbol{X}) = D_{\text{poles}}/D_{\text{poles},0} - 1.25 \leq 0 \tag{5}$$

where $D_{\text{poles},0}$ and $D_{\text{poles},0}$ are, respectively, the minimum distance from the level 1 boundary of the poles of the optimized and of the baseline design. The level 1 boundary is that of the specification chart in Sec. 3.3.2.3 of ADS-33 (Ref. 8).

Rotor Dynamics Constraint

The fourth constraint is that the rotor modes must be stable. This constraint on the stability of all of the rotor modes is implemented with one inequality, which requires that the damping ratio of the least damped mode be positive, that is,

$$g(\boldsymbol{X}) = -\zeta/0.01 \leq 0 \tag{6}$$

where 0.01 is a scaling factor. Typically, the mode with the smallest damping ratio ζ is the higher frequency first progressive lag mode, but the constraint is enforced for the least damped rotor mode regardless of type.

Optimization Case 2

For this optimization, the behavior constraints include those that require the time integration of the nonlinear equations of motion. Therefore, the behavior constraints include all of those of case 1 plus the following.

Handling Qualities Constraints

The fifth constraint is level 1 quickness in pitch. This constraint is implemented on the basis of the specification chart of Sec. 3.3.3 of ADS-33 (Ref. 8) for the MTE, for moderate amplitude attitude changes. The distance $D_{\text{pitch},m}$ of the point representative of the helicopter from the level 1 boundary ($D_{\text{pitch},m}$ negative if the point is in the level 1 region) must be negative:

$$g(\boldsymbol{X}) = D_{\text{pitch},m} \leq 0 \tag{7}$$

The sixth constraint is level 1 quickness in roll. Similarly to the pitch constraint,

$$g(\boldsymbol{X}) = D_{\text{roll},m} \leq 0 \tag{8}$$

The seventh constraint is roll-to-pitch coupling equal to 125% of the baseline or better. This interaxis-coupling constraint is defined in terms of the roll-to-pitch coupling $p_{\text{pk}}/q_{\text{pk}}$ during the same pitch maneuver used for the pitch quickness constraint, that is,

$$g(\boldsymbol{X}) = \frac{p_{\text{pk}}/q_{\text{pk}}}{[p_{\text{pk}}/q_{\text{pk}}]_0} - 1.25 \leq 0 \tag{9}$$

where $[p_{\text{pk}}/q_{\text{pk}}]_0$ denote the interaxis coupling for the baseline configuration. This is a simpler and less restrictive version of the ADS-33 interaxis coupling constraint, from which it differs in two ways: (1) To reduce the computational effort, the same maneuver as in the calculation of the pitch quickness constraint is used, rather than the specific step input called for by ADS-33. (2) The limit of the peak pitch-to-roll rates ratio is defined relative to the baseline configuration, rather than in absolute terms as in ADS-33, because the simple flight control system used in the present study has no crossfeeds, and therefore, the original ADS-33 constraint may be too stringent. These simplifications are probably reasonable given the scope of the present study.

The eigth constraint is pitch-to-roll coupling equal to 125% of the baseline or better. This constraint is the same as the preceding one, except that it is evaluated from the maneuver used for the roll quickness calculations. The constraint is implemented as

$$g(\boldsymbol{X}) = \frac{q_{\text{pk}}/p_{\text{pk}}}{[q_{\text{pk}}/p_{\text{pk}}]_0} - 1.25 \leq 0 \tag{10}$$

where $[q_{\text{pk}}/p_{\text{pk}}]_0$ denote the interaxis coupling for the baseline configuration.

The ninth constraint is pitch attitude change for quickness calculations between 20 and 30 deg. The constraint is

$$20 \text{ deg} \leq \Delta\theta_{\min} \leq 30 \text{ deg} \tag{11}$$

and is implemented in the form

$$g(\boldsymbol{X}) = 1 - \Delta\theta_{\min}/20 \leq 0, \qquad g(\boldsymbol{X}) = \Delta\theta_{\min}/30 - 1 \leq 0 \tag{12}$$

This constraint fixes the range of attitude angles used for the calculation of the quickness constraint. This implies two simplifications. The first is that the quickness calculations are not strictly performed for the same attitude change. The second is that, although the quickness constraint should be evaluated for several values of the attitude changes, covering the entire range of moderate amplitude attitude changes, for simplicity, in the present study the evaluation will be limited to just one value of $\Delta\theta_{\min}$.

The 10th constraint is roll attitude change for quickness calculations between 30 and 50 deg. This constraint is similar to the preceding one and is defined as

$$30 \text{ deg} \leq \Delta\phi_{\min} \leq 50 \text{ deg} \tag{13}$$

and implemented as

$$g(\boldsymbol{X}) = 1 - \Delta\phi_{\min}/30 \leq 0, \qquad g(\boldsymbol{X}) = \Delta\phi_{\min}/50 - 1 \leq 0 \tag{14}$$

Rotor Dynamics

The 11th constraint is hub load increase during pitch maneuver equal to 125% of the baseline or better. The hub loads constraints are defined with the use of a load function F_{hub} defined as

$$F_{\text{hub}} = \sqrt{X^2 + Y^2 + Z^2 + K^2(L^2 + M^2 + N^2)} \tag{15}$$

where X, Y, Z, L, M, and N are the forces and moments acting on the hub and K is a scaling constant that makes the numerical values of the hub forces comparable to those of the hub moments. All forces and moments in Eq. (15) are generally time dependent. Then, a quantity ΔF_{hub} is the defined as the difference between the maximum value of F_{hub} during a maneuver and the maximum value of F_{hub} at trim (where F_{hub} will usually be time dependent in both cases), that is,

$$\Delta F_{\text{hub}} = \max|F_{\text{hub}}(t)| - \max|F_{\text{hub}}(t=0)| \tag{16}$$

The specific maneuver used in the evaluation of this constraint is the same maneuver used to evaluate the pitch quickness constraint. Note that, in general, both terms in Eq. (16) will be a function of the design variable vector $\boldsymbol{X}$. The baseline time integration will have its own value of ΔF_{hub} that will be denoted ΔF_{hub_0}. The hub load constraint limits the maximum variation of hub load acting on the helicopter during the maneuver and is implemented as

$$g(\boldsymbol{X}) = \Delta F_{\text{hub}} \big/ \Delta F_{\text{hub}_0} - 1.25 \leq 0 \tag{17}$$

where ΔF_{hub_0} is the value corresponding to the baseline design. Therefore, the increase in hub loads, ΔF_{hub}, during the maneuver (compared with trim) cannot be greater than 25% of the same increase for the baseline configuration. Originally, this constraint was formulated in terms of peak-to-peak hub loads during the maneuver, but preliminary calculations showed that the peaks could not be always identified unambiguously.

Design Optimization Procedure

All optimizations are carried out using the modified method of feasible directions[19] as implemented in the optimization code DOT.[20] In all cases, the procedure begins by trimming the helicopter and computing objective function and behavior constraints for the initial configuration. The initial design is feasible.

For optimization case 1 (objective and constraints from linearized model only) and finite difference-based gradients, forward finite differences are used for both objective function and behavior constraints. Trim condition and blade modes are recalculated for every new design if necessary, including the perturbed designs needed for finite difference calculations. (Some design variables do not affect trim or blade modes.) For case 1 with semi-analytical gradients, the analysis provides both the baseline values of objective function and constraints, as well as their gradients with respect to each of the design variables if necessary. Recall that most gradient-based optimization algorithms, including the one used in the present study, proceed by repeatedly performing two steps.[19] The first, that is, the definition of a direction of descent, requires gradient calculations, whereas the second, that is, the one-dimensional minimization along the direction of descent, does not. For case 1 with semi-analytical gradients, trim and blade mode shapes are recalculated for each design selected during the one-dimensional minimization, but the semi-analytical gradients themselves do not take trim or mode changes into account.

For optimization case 2 (all constraints), the gradients of the objective function and of those behavior constraints that are computed from the linearized model are calculated semi-analytically. The gradients of the constraints that require the integration of the nonlinear equations of motion are computed using forward finite difference approximations, which also take into account changes in trim and mode shapes. During the one-dimensional minimization, changes in trim and mode shapes are taken into account for the objective function and all of the constraints.

Some additional assumptions, not described in the preceding section, are made in the evaluation of the quickness constraints. First, the pilot input is held fixed throughout the optimization, and therefore, the maneuvers for different designs are not strictly equivalent. Second, only one maneuver is considered for pitch and one for roll; therefore, the maneuvers are not necessarily optimal, that is, they do not necessarily produce the maximum values of roll and pitch rates p_{pk} or q_{pk} for a given value of $\Delta\theta_{\min}$. Finally, the quickness criteria require that the pilot maintain a constant attitude after the maneuver for at least a few seconds. In the present study, this is strictly true for the initial design only. Because the pilot control input is held fixed, design parameter variations can affect time histories, especially at the end of the maneuver. Therefore, the quickness specification parameters, (for example, q_{pk}, $\Delta\theta_{\min}$, $\Delta\theta_{\text{pk}}$, etc.) are calculated based on only the first 3 s of the time histories of the integration, whether or not the attitude has stabilized at that point (or has stabilized at all).

Results

Initial Design

The initial helicopter configuration used in this study is similar to a Eurocopter BO-105, flying at 40 kn with $C_T/\sigma = 0.07$. The initial configuration has all of the flight control system gains set to zero (bare airframe configuration). The initial design has level 1 handling qualities for almost all of the small amplitude and moderate amplitude attitude changes criteria considered in this study. The only exception is the midterm response, Paragraph 3.3.2.3.1 of ADS-33 (Ref. 8), which is level 2 because of the position of the Dutch roll pole. The initial value of the objective function, that is, the damping of the progressive lag mode, is 4.49% of the critical damping.

Optimization Case 1

For this case, only the behavior constraints obtained from the linearized model of the helicopter are retained. The constraints that require the integration of the nonlinear equations of motion are not included.

Before focusing on this case, it may be interesting to discuss some results of a preliminary study. In an attempt to also obtain level 1 handling qualities for the Dutch roll, optimization case 1 was run using the distance of the Dutch roll pole from the level 1 boundary as the objective function to be minimized. It was hoped that the optimizer would reduce this distance to the point of moving the Dutch roll pole at least on the level 1 boundary. The initial optimization run for this modified case terminated after making negligible progress. All of the local convergence tests were satisfied, but the optimum design was almost identical to the initial design. Figure 1 shows the reason for this unsuccessful attempt.

The first step of the optimization consists of obtaining the gradient of the objective function, which is then used as the first search direction to minimize the objective function. The gradient is also used[19] to estimate the relative and absolute change in the design variables that will provide a desired reduction of the objective function. These estimates are then used to determine the initial move in the one-dimensional search. With the standard values of the optimizer settings and with the design variables considered in this problem, the suggested absolute changes in the design variables were very small. The optimizer seemed to find a one-dimensional optimum very close to the initial design, and a further exploration of that region seemed to indicate that the objective function was nonsmooth and nonconvex in that direction, with at least two relative minima, as shown in Fig. 1a.

The quantity on the x axis of Figs. 1a and 1b is the step size α in the descent direction. The values $0 \leq \alpha \leq 3$ shown in Fig. 1a correspond to extremely small design changes, of the order of 0.1% or less. When more realistic values of α, that is, $0 \leq \alpha \leq 2000$, were considered, the objective function looked quite smooth and well behaved, as shown in Fig. 1b. Simple adjustments of the optimizer settings, such as increasing the step size for finite difference gradient calculations from 0.01 to 1% and increasing the maximum relative and absolute changes in the design variables and in the objective functions in the first iteration from 0.1 to 0.2 and 0.5, respectively, greatly improved the behavior of the one-dimensional minimizations. Then, the Dutch roll pole could be moved closer to (although still outside) the level 1 region. These preliminary results show the need to examine critically the results of an optimization and confirm that a design optimization computer program should never be used as a black box.

Table 2 shows the results of optimization case 1. Two sets of results are presented, one for the case of finite difference-based gradients and the other for semi-analytical gradients. The damping ratio of the progressive lag is increased to about 8.5% for both cases. This corresponds to an increase of about 90% from its baseline value. Table 2 shows that the two procedures produce very similar results: The differences in optimum design variables are always less than 1%. The discrepancies relative to the pitch and roll rate feedback may appear large: The optimum values for the optimization with finite difference gradients are zero, whereas those for the optimization with semi-analytical gradients are equal to about 2.4 and 3.4, respectively. However, note that the range for the flight control system gains is large, between 0 and 300, and therefore, those differences are not significant. Also, the effects of such small amounts of feedback are probably negligible: $K_p = 3.4$ means that the flight control system reacts to a roll rate of 1 rad/s (or about 57 deg/s) with a lateral input in the opposite direction of 3.4% of the total stick excursion.

The optimum design is feasible. The handling qualities remain level 1 for pitch and roll bandwidth, despite some deterioration in the pitch degree of freedom. The rotor also remains stable, although the damping ratio of the least damped mode is a relatively low 1.65%. This indicates that the objective function should probably be reformulated to maximize the damping ratio of the least damped rotor mode, regardless of type, or that the constraint on rotor damping should be tightened, and require that the damping of the least damped mode does not decrease during the optimization.

The parameter that most affects the objective function, that is, the damping of the progressive lag mode is the torsional stiffness GJ. In both cases, the side constraint on the torsional stiffness is active,

Table 2 Results for optimization case 1 linearized system constraints only

Quantities	Baseline	Optimized	
		Finite difference gradients	Analytical gradients
Objective function ζ, %	4.49	8.53	8.45
Design variables			
$X_1 = \Delta S_H / S_H$	0	−0.0006	0.0005
$X_2 = \Delta GJ / GJ$	0	−0.5000	−0.5000
$X_3 = \Delta x_i / c(\%)$	0	−0.1495	−0.1759
$X_4 = \Delta c / c_0$	0	−0.0501	−0.0394
$X_5 = K_\theta$, %/rad	0	0.6464	1.0645
$X_6 = K_q$, %s/rad	0	0.0000	2.4083
$X_7 = K_\phi$, %/rad	0	1.2584	2.0751
$X_8 = K_p$, %s/rad	0	0.0000	3.4191
Constraint values			
$g_1(\boldsymbol{X}) = D_{\text{pitch}}$ small amplitude	−2.10	−0.57	−0.71
$g_2(\boldsymbol{X}) = D_{\text{roll}}$ small amplitude	−0.98	−1.02	−1.03
$g_3(\boldsymbol{X}) = D_{\text{oscill}}$	0.24	0.23	0.24
$g_4(\boldsymbol{X})$ = minimum rotor damping	1.65	1.65	1.65

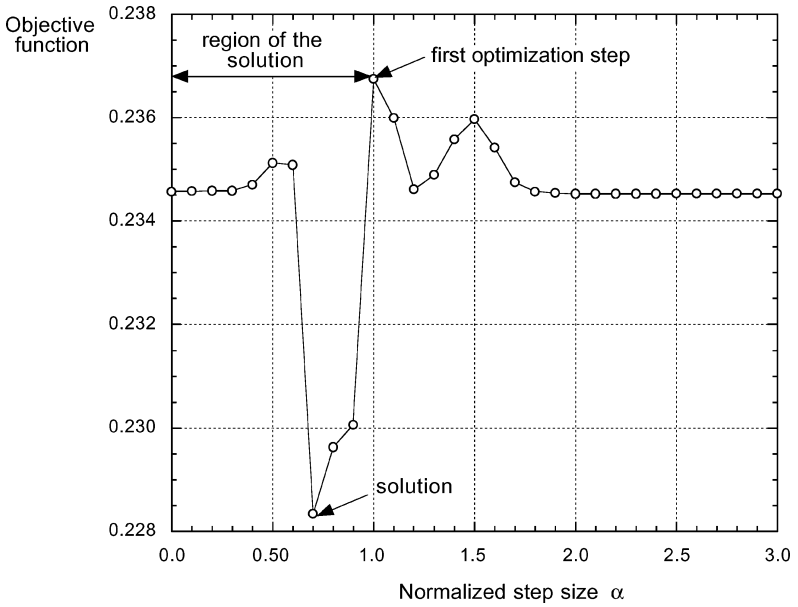

Fig. 1a Objective function: detail of the region close to the origin.

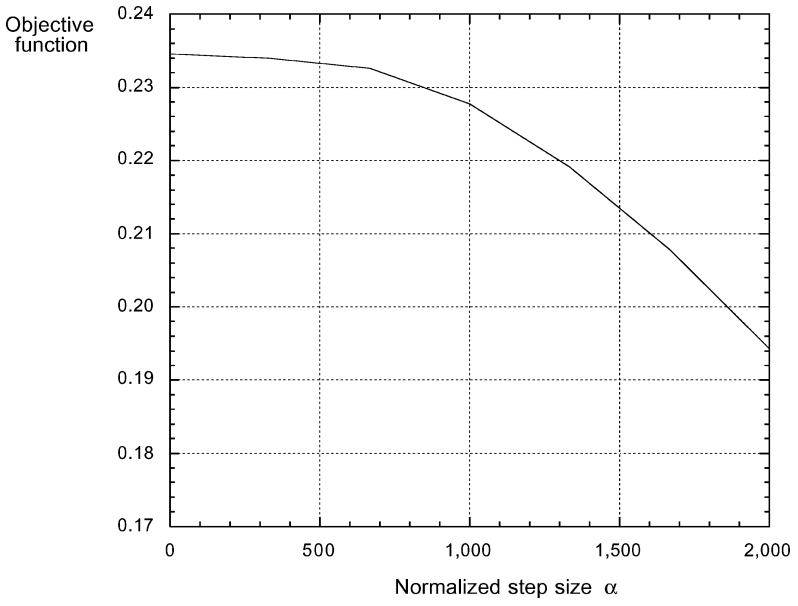

Fig. 1b Objective function value along the search direction of the first step of the optimization.

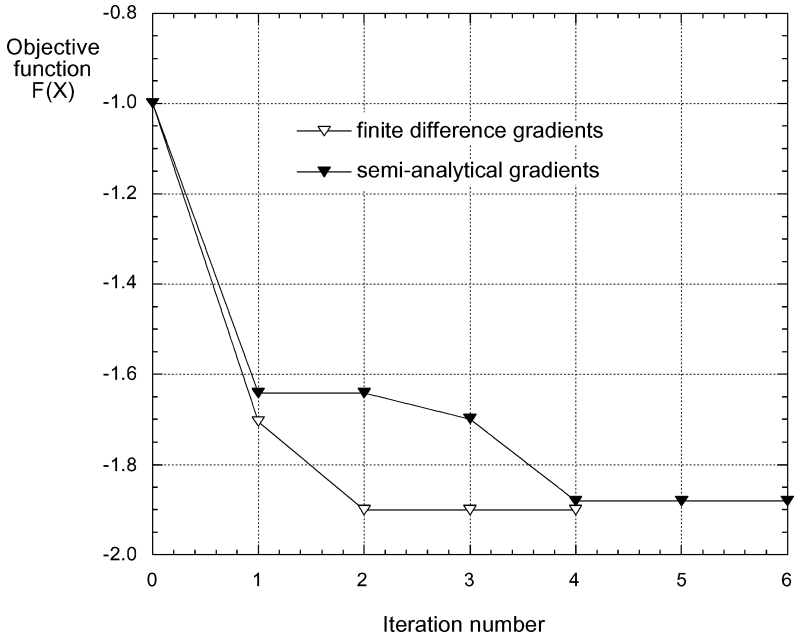

Fig. 2 Iteration history of the objective function, optimization case 1.

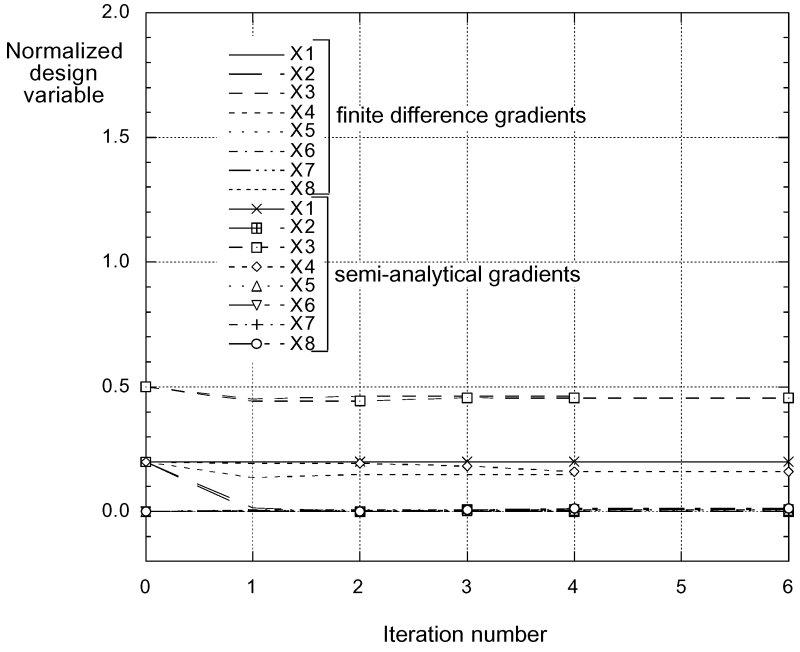

Fig. 3 Iteration history of design variables, optimization case 1.

and *GJ* is 50% of its initial value. All of the other parameters change very little, if at all, with respect to their initial values.

The iteration history of the objective function $F(\boldsymbol{X}) = -\varsigma/\varsigma_0$ is shown in Fig. 2. Four iterations are needed to reach the optimum when the gradients are calculated using finite different approximations vs six when semi-analytical gradients are used. The likely reason is that the semi-analytical gradients are calculated for fixed trim and blade mode shapes and, therefore, are approximate. In turn, this influences the accuracy of the search directions and, ultimately, the number of one-dimensional searches required.

Despite the higher number of one-dimensional minimizations, the optimization with semi-analytical gradients is still the less computationally intensive. In fact, it requires 29 evaluations of the objective function and constraints vs 48 when finite difference gradients are used, for an improvement of about 40%. In the first case, 6 of the 29 function evaluations include the calculation of the gradients (which increases the computational cost by about 20–25%), with the remaining 23 needed for the 6 one-dimensional minimizations. In the second case, 36 of the 48 function evaluations are used to compute baseline values and gradients for the 4 calculations of the search directions, with the remaining 12 needed for the 4 one-dimensional minimizations. In other words, the additional work required for the larger number of one-dimensional minimizations is more than compensated by the much faster gradient calculations. In general, the efficiency will increase even more as the number of design variables increases.

Figure 3 shows the iteration history of the eight design variables. (Recall that the variables are normalized such that they are equal

to 0 at their lower bound and to 1 at their upper bound.) The key design change, namely, the reduction of the torsion stiffness GJ, occurs during the first iteration of the optimization. Much smaller changes occur in subsequent iterations. Figure 4 shows the iteration history of the behavior constraints $g_j(\boldsymbol{X})$, $j = 1, \ldots, 4$. All of the behavior constraints are satisfied in the initial design and remain so as the optimization progresses. The representative point on the pitch bandwidth chart moves noticeably closer to the level 1 boundary, but stays well inside the level 1 region.

Considering the overall results of this optimization, it is clear that the flight control system design variables and the ADS-33-based constraints play a minor role. The increase in damping of the least damped mode (in the initial design), that is, the progressive lag mode is obtained through a reduction in torsional stiffness. The governing physical mechanism is likely an increase in lag aerodynamic damping due to the increased torsional deformations and consequent increase in aerodynamic drag. In the absence of other constraints, such as vibratory loads or required power, what prevents the torsion stiffness from decreasing further is the corresponding side constraint, which is the only constraint active at the optimum. In particular, the rotor stability constraints remain satisfied; however, by simply requiring that the rotor be stable rather than enforcing a minimum damping level, these constraints might be too forgiving. The increase in progressive lag mode, even if perhaps optimistic given the preceding considerations, is significant, because the damping ratio almost doubles. From a computational standpoint, optimizing using semi-analytical or finite difference-based gradients produces very similar results, but the former approach is substantially more efficient.

Optimization Case 2

For this case, both the behavior constraints obtained from the linearized model of the helicopter and those that require the integration of the nonlinear equations of motion are included. The gradients of objective function and linearized model constraints are calculated using a semi-analytical method; those from the nonlinear model are calculated using finite difference approximations.

The results of the optimization are summarized in Table 3. The damping ratio of the progressive lag mode is increased to $\zeta = 6.34\%$, which corresponds to an increase of about 41% from its baseline value. The optimum design is feasible, and two constraints are active at the optimum, namely, the behavior constraint enforcing level 1 handling qualities for the pitch quickness criterion and the side constraint enforcing a lower bound on the pitch rate feedback to longitudinal cyclic. As in optimization case 1, the primary design change produced by the optimizer is a reduction of the blade torsion stiffness. However, in this case the reduction is of only 37%, and torsion stiffness does not reach its lower bound as in case 1 because the pitch quickness constraint becomes active first. Compared with case 1 results, the flight control system gains are slightly higher, the horizontal tail is slightly larger, and there is a small rearward shift of the cross-sectional blade c.g. location, but overall, the design changes other than torsion stiffness are quite small.

Figure 5 shows the locations of all of the poles for the baseline and the optimized configuration. For the baseline configuration the fundamental torsion mode has a frequency of about 3/per revolution, which decreases to about 2.4/per revolution in the optimized configuration. As in case 1, it is possible that with additional required power or vibratory load constraints the torsion frequency would not be allowed to decrease to such small values.

The rigid-body poles are shown again in Fig. 6, this time with the handling qualities level boundaries from the ADS-33F criteria.

Table 3 Results for optimization case 2

Quantities	Baseline	Optimized
Objective function ζ, %	4.49	6.34
Design variables		
$X_1 = \Delta S_H / S_H$	0	0.0298
$X_2 = \Delta GJ / GJ$	0	−0.3687
$X_3 = \Delta x_i / c$, %	0	−0.1588
$X_4 = \Delta c / c_0$	0	−0.0318
$X_5 = K_\theta$, %/rad	0	0.0000
$X_6 = K_q$, %s/rad	0	8.8317
$X_7 = K_\phi$, %/rad	0	2.1155
$X_8 = K_p$, %s/rad	0	3.7497
Constrained quantities		
D_{pitch} small amplitude	−2.10	−1.50
D_{roll} small amplitude	−0.98	−1.01
D_{oscill}	0.24	0.23
$D_{\text{pitch},m}$ moderate amplitude	−1.12	0.00
$D_{\text{roll},m}$ moderate amplitude	−3.75	−3.22
$q_{\text{pk}}/p_{\text{pk}}$ for roll maneuver	0.18	0.23
$p_{\text{pk}}/q_{\text{pk}}$ for pitch maneuver	0.24	0.30
$\Delta\theta_{\min}$, deg	23.33	20.48
$\Delta\phi_{\min}$, deg	39.11	36.40
ΔF_{hub} pitch, lb	1387	1164
ΔF_{hub} roll, lb	9879	9364

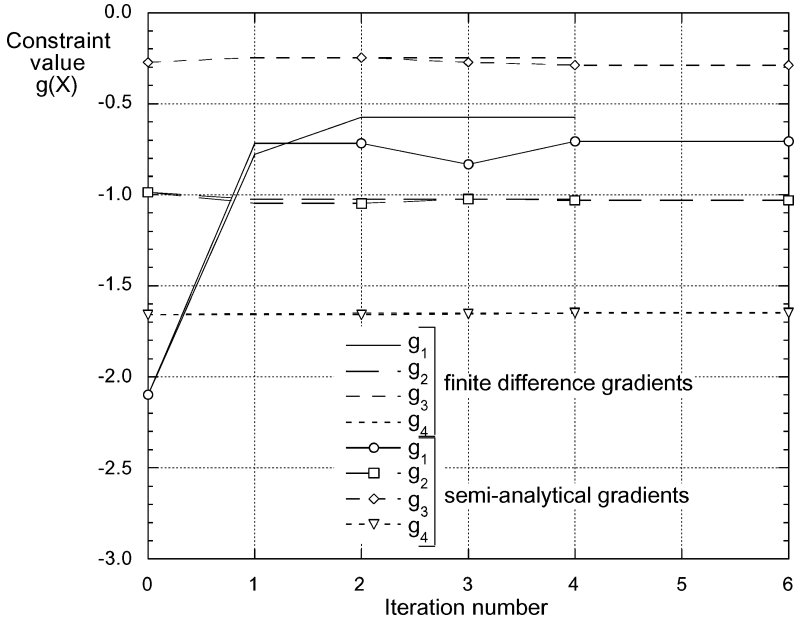

Fig. 4 Iteration history of behavior constraints with finite difference and semi-analytical gradients, optimization case 1.

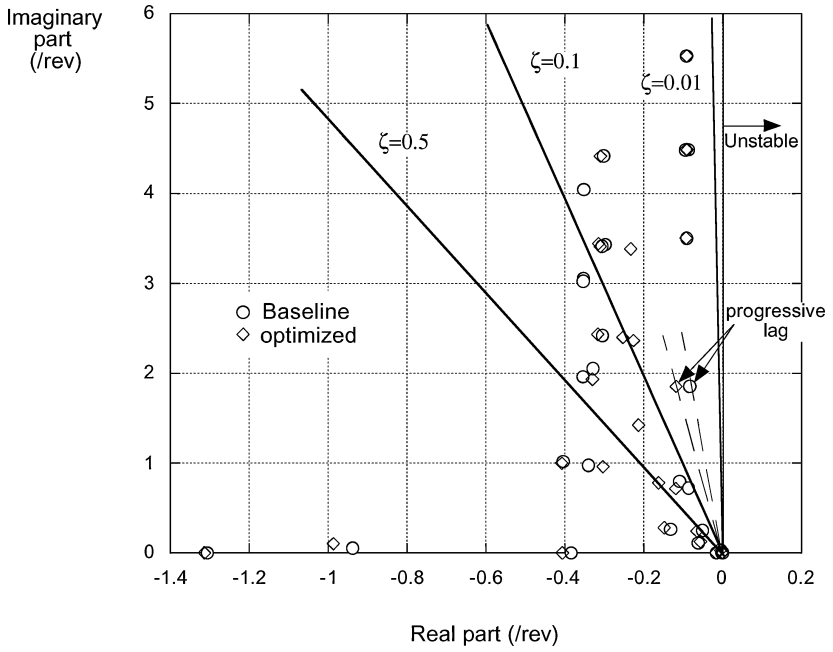

Fig. 5 Rotor poles for baseline and optimized configuration.

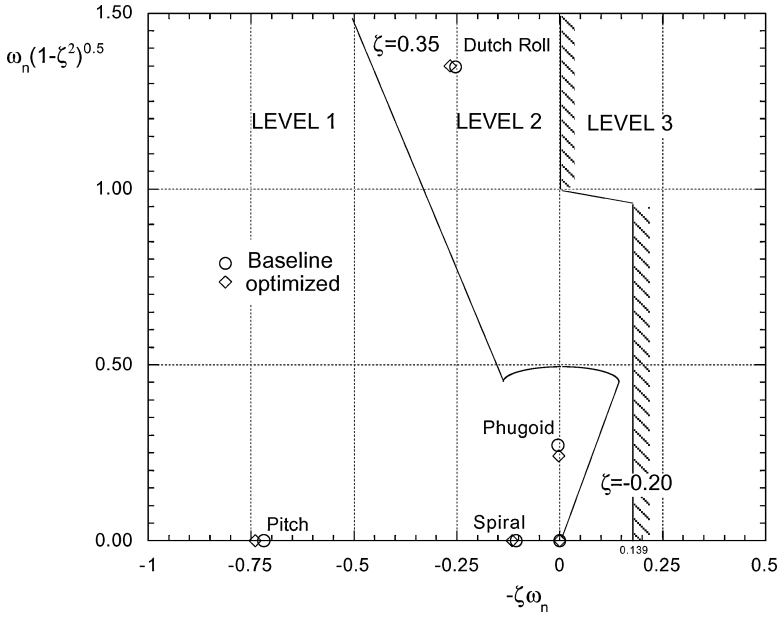

Fig. 6 Rigid-body poles for baseline and optimized configurations.

Recall that preliminary optimizations had shown that it would not be possible to move the Dutch roll poles to the left of the level 1 boundary with just the design parameters used in the study. Therefore, the constraint simply required that the damping of the Dutch roll pole would not decrease during the optimization. With this in mind, all of the constraints on the rigid-body poles are clearly satisfied.

Figures 7 and 8 show the representative points of the baseline and optimum designs on the ADS-33 chart for bandwidth/phase delay for the pitch and roll axes, respectively. Figure 7 shows that the optimum design is characterized by smaller values of pitch bandwidth ω_{BW} and phase delay $\tau_p$than the baseline. The pitch decreases from $\omega_{\mathrm{BW}} = 4.1$ rad/s to $\omega_{\mathrm{BW}} = 3.5$ rad/s. Figure 7 shows a small negative value of phase delay for the optimum design. This result, which is not physically meaningful because it would imply that the helicopter anticipates the pilot action, is an artifact of the procedure to compute the phase delay. In fact, the frequency response phase curve is strongly nonlinear between the ω_{180} and $2\omega_{180}$ frequencies because of the presence of a rotor mode. When this occurs, ADS-33 prescribes that the phase delay be computed from a linear least-squares fit of the phase curve between those frequencies, rather than from the phase curve itself. In the optimum design, the linear fit is such that applying the ADS-33 prescribed procedure leads to the slightly negative phase delay shown in Fig. 7. This result means that the increase of the progressive lag damping is obtained with a small deterioration of the pitch handling qualities, which, however,

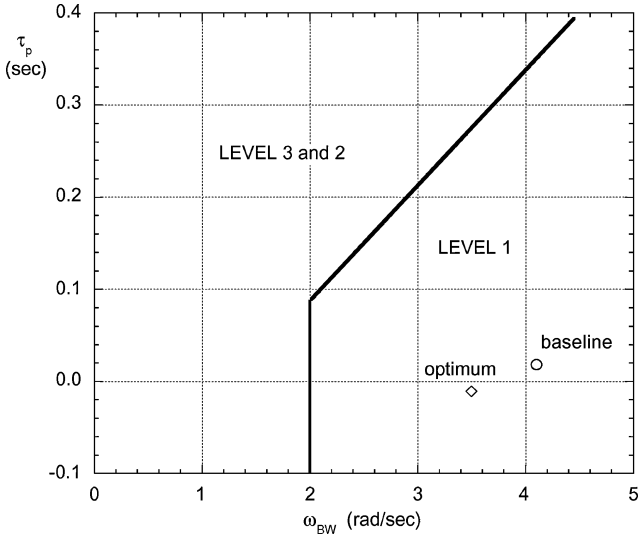

Fig. 7 ADS-33 small amplitude attitude changes (pitch); baseline and optimized configurations (Sec. 3.3.2.1, Ref. 8).

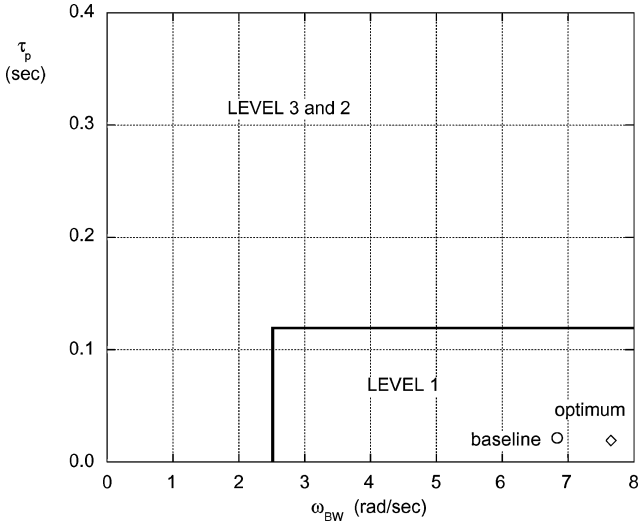

Fig. 8 ADS-33 small amplitude attitude changes (roll); baseline and optimized configurations (Sec. 3.3.2.1, Ref. 8).

remain level 1. Figure 8 shows the corresponding chart for the roll axis. Here, the optimum design has roughly the same delay and a slightly higher bandwidth compared with the baseline. When Figs. 7 and 8 are examined, note that the simulation model does not include any actuator or computation delays. As a consequence, the delay values in Fig. 8 are optimistic, although not enough as to modify the conclusions of this study.

Figures 9 and 10 show the representative points of the baseline and optimized designs on the ADS-33 compliance charts for the quickness specifications. Figure 9 refers to the pitch quickness. For the baseline configuration, the attitude change $\Delta\theta_{\min}$ is about 23 deg with the peak pitch rate to peak pitch attitude ratio $q_{\text{pk}}/\theta_{\text{pk}}$ of about 1.2/s, which place the configuration well within the level 1 region. The optimum design is on the level 1 boundary, with a value of $\theta_{\min}$ of about 21 deg. Therefore, the pitch quickness constraint is active. Note that the attitude change $\Delta\theta_{\min}$ is not necessarily constant during the optimization. Recall that the pilot input, which is added to the trim values of the controls, is held constant during the optimization. Furthermore, the trim state is recalculated for each updated design. The effects of the design changes and of the trim update, combined with the fixed perturbation pilot input, result in a total pilot input that usually produces different attitude changes as the optimization progresses. A more rigorous approach would require that the attitude change $\Delta\theta_{\min}$ remain constant during the optimization and that the pilot input vary accordingly. This constant $\Delta\theta_{\min}$ approach is computationally much more intensive because it requires the use of inverse simulation techniques and will be left for future research. Finally, note that, although actuator displacement or rate saturation are often the limiting factor in achieving level 1 quickness handling qualities, neither was taken into account in the present study. However, no saturation was encountered in the cases of this study and, in any case, saturation can easily be added to the optimization in the form of inequality constraints on the time histories of the pilot inputs. Figure 10 shows the representative points of the baseline and optimized designs on the ADS-33 compliance charts for the roll quickness specification. Both designs have level 1 handling qualities. The earlier considerations on the $\Delta\theta_{\min}$ changes apply to the roll axis and $\Delta\ \phi_{\min}$. Actuator saturation is again neglected, but never occurred in this optimization.

Finally, Figs. 11 and 12 show, respectively, the time histories of the hub load parameter F_{hub} during the pitch and the roll maneuvers carried out to verify compliance with the quickness specifications. The quantity F_{hub} was defined in Eq. (15) as the root mean square of the sum of the instantaneous hub forces and moments (the latter multiplied by an arbitrary constant to have forces and moments of the same order of magnitude). In both cases, F_{hub} increases during the maneuver, primarily, because the rotor needs to generate the pitch and roll moments required to accomplish the attitude changes. There is no requirement that the maneuver be carried out at constant altitude, and therefore, there is no need to adjust rotor thrust accordingly. The hub load constraints limit the value of the maximum variation of the hub loads ΔF_{hub}, compared with trim, to a maximum of 125% of the baseline value ΔF_{hub_0}. Figure 11 shows the time histories of ΔF_{hub} for the pitch maneuver. The optimum design has a noticeably lower F_{hub} peak than the baseline design and slightly higher value in the later portions of the maneuver. Recall that the primary difference between the two designs is a lower value of the blade torsion stiffness for the optimum design and that the pitch quickness constraint is active at the optimum. Therefore, if the torsion stiffness cannot be lowered further, it is not because the loads during the pitch maneuver become too high; a more likely reason is some intrinsic rotor limitation, such as the inability to generate enough pitching moments, possibly due to stall. Figure 12 shows the time histories of ΔF_{hub} for the roll maneuver. The baseline and the optimized configuration have approximately the same hub loads (as collapsed in the F_{hub} parameter) throughout the maneuver, with a small reduction for the optimized configuration.

The results of this optimization clearly show that there is a significant interaction between rotor dynamics and flight dynamics. In fact, the optimizer increases the damping of the progressive lag mode primarily by reducing the torsion stiffness of the blade, but the improvements end up being limited by a flight dynamics-type constraint, namely, the need to maintain level 1 handling qualities for the pitch quickness criterion of ADS-33.

From a computational viewpoint, the most demanding portion of the optimization was by far the calculation of the time histories for the pitch and roll quickness maneuver. Recall that all of the gradients of the constraints associated with this maneuver were calculated using one-sided, forward finite difference approximations. The six iterations required to perform the optimization required computer times of the order of 100 h on typical desktop computers, with over 85% of the time required for the pitch and roll maneuvers. Because the time histories needed for gradient calculations can be obtained independently of one another, an order of magnitude reduction in elapsed time can probably be achieved by exploiting parallelism. A further reduction by a factor of 2–4 could also be achieved by using faster computing hardware. Finally, further gains are possible by improving the simulation code, which was not optimized for execution time. On the other hand, the optimization problem described in this section has a small number of design variables and behavior constraints. Although this small size is sufficient to highlight basic concepts, a realistic design application would require many more design variables and constraints, and the computational requirements would grow accordingly. Therefore, both advances in computer hardware and in optimization algorithms, including

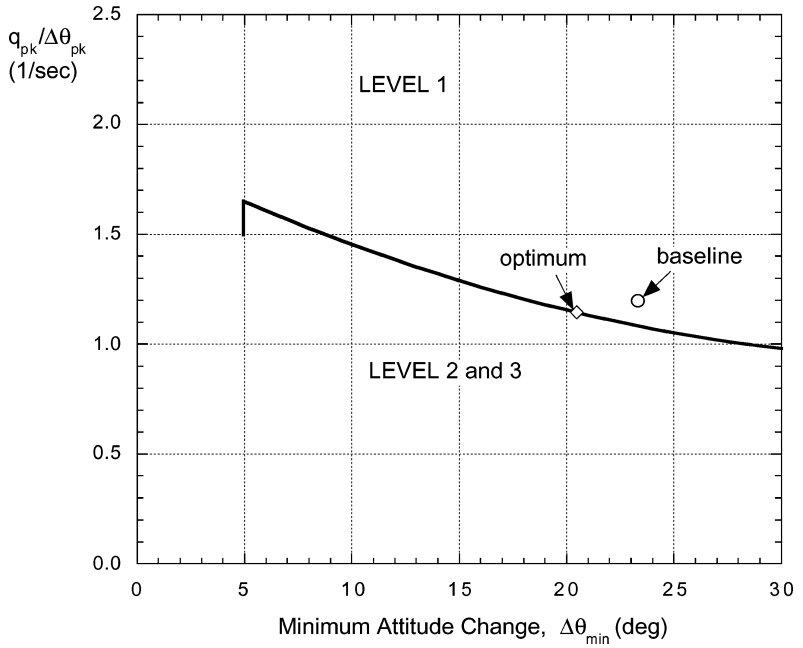

Fig. 9 ADS-33 moderate amplitude attitude changes (pitch); baseline and optimized configurations (Sec. 3.3.3, Ref. 8).

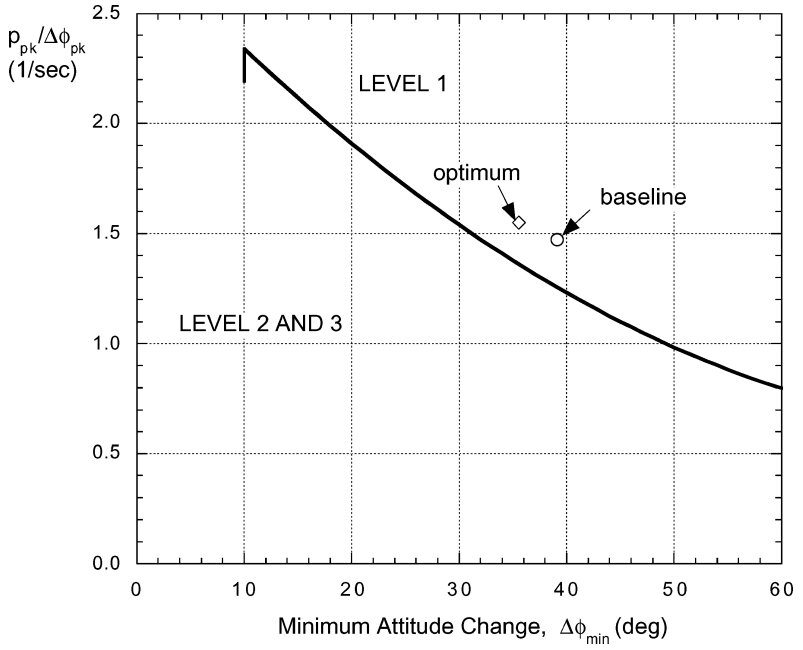

Fig. 10 ADS-33 moderate amplitude attitude changes (roll); baseline and optimized configurations (Sec. 3.3.3, Ref. 8).

efficient sensitivity analyses, will be required to make numerical optimization a practical design tool.

Limitations of the Present Study

The key accomplishments of the present study consist of (1) providing clear quantitative evidence that the aeromechanical design problem is multidisciplinary and (2) describing a systematic, optimization-based methodology to carry out this design, which is applicable to simulation models of realistic complexity, that is, is not limited to simplified models. However, the study also has several important limitations that should be kept in mind when one tries to extend and generalize its conclusions. Some limitations have been already mentioned in earlier portions of this paper; additional ones are now listed.

First, although both design variables and behavior constraints were representative of many key areas of the aircraft design and aeromechanical behavior, the number of each was small. For example, only three rotor design variables were used, and the flight control system was rudimentary, both in structure and in the number of design variables.

Second, only one flight condition was taken into account, that is, the issue of the robustness of the final design was not addressed. Previous studies[6,7] have shown that optimization-based procedures can produce designs that are excellent for the specific flight condition for which the optimization has been carried out, but that violate one or more constraints in other flight conditions. Taking other flight conditions simultaneously into account reduces this problem, but also reduces the achievable improvements.

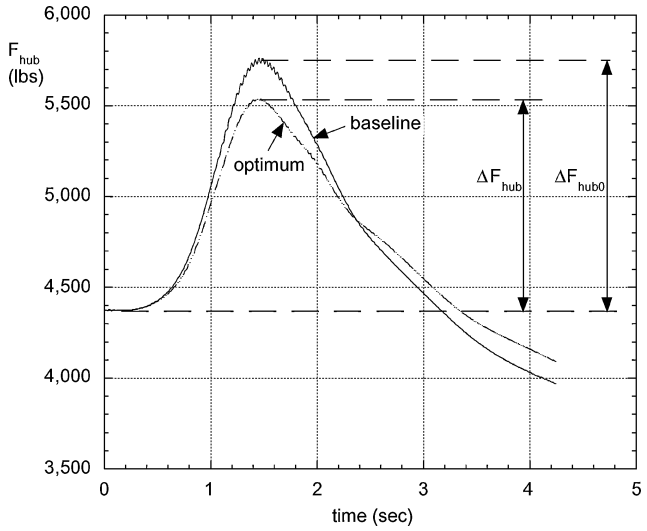

Fig. 11 Hub loads function F_{hub} for the pitch quickness maneuver; baseline and optimized configurations.

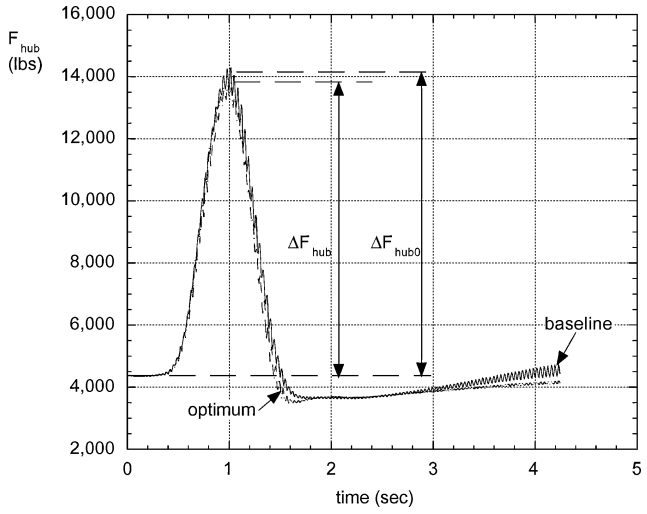

Fig. 12 Hub loads function F_{hub} for the roll quickness maneuver; baseline and optimized configurations.

Finally, although the baseline configuration used in this study was realistic, it did not exhibit some aeromechanic problems that could generate tradeoffs between rotor dynamics and flight dynamics. For example, the bare airframe configuration already had level 1 handling qualities with respect to the bandwidth/phase delay ADS-33 criteria. Therefore, it was not necessary to increase the gains of the flight control system (within the simple architecture used in this study), which, in turn, could have destabilized one or more of the rotor modes.

Conclusions

This paper presented a multidisciplinary design optimization study, in which both rotor dynamics and flight dynamics were simultaneously taken into account. The objective was to maximize the damping ratio of the least damped rotor mode in the baseline configuration, namely, the lag progressive mode. The eight design variables comprised rotor, airframe, and flight control system parameters. The behavior constraints included rotor stability, rotor loads, and several ADS-33-based handling qualities constraints. The 53-state simulation model included flexible blade dynamics and a detailed representation of fuselage and empennage. The baseline design was a hingeless rotor helicopter similar to the BO-105. Two design optimization cases were considered. The first, case 1, had only constraints computed from the linearized model of the helicopter. In this case, the optimization was repeated twice, once with gradients of objective function and behavior constraints obtained using finite difference approximations and once with gradients obtained with a more efficient semi-analytical technique. The second case, case 2, also included constraints that required the integration of the nonlinear equations of motion, with the gradients of these constraints computed using finite difference approximations. Several simplifications were made in the optimization process and were discussed in the paper: These simplification should be carefully reviewed to determine the applicability of the conclusions that follow to other helicopter design problems.

The main conclusions of the present study are as follows.

1) For the baseline configuration of this study, and in both cases, the optimization procedure managed to increase the progressive lag mode damping by up to 90%. The final design satisfied all constraints. In both cases, this was achieved primarily by reducing the torsion stiffness of the blade.

2) The aeromechanic design problem is a multidisciplinary problem. This is especially evident in the case 2 optimization, where the constraint active at the optimum (and, therefore, the limit to further improvements in lag damping) was the level 1 handling qualities requirement in the pitch axis. Optimization-based design provides a framework to manage multidisciplinary problems in a systematic and efficient way.

3) Using the approximate, but very efficient semi-analytical gradients of the constraints computed from the linearized model yields the same results as with finite difference gradients. More iterations of the optimization process are needed, but this is more than compensated by the much faster gradient calculations. The computational advantage will increase with problem size.

4) From a computational viewpoint, the calculation of constraints that require the time histories of the response to pilot inputs is by far the most time consuming portion of the optimization. Therefore, both advances in computer hardware and in optimization algorithms, including efficient sensitivity analyses, will be required to make numerical optimization a practical design tool.

Acknowledgments

This research was supported by the National Rotorcraft Technology Center under the Rotorcraft Center of Excellence Program, Technical Monitor, Y. Yu.

References

[1]Friedmann, P. P., "Helicopter Vibration Reduction Using Structural Optimization with Aeroelastic/Multidisciplinary Constraints—A Survey," *Journal of Aircraft*, Vol. 28, No. 1, 1991, pp. 8–21.

[2]Adelman, H. M., and Mantay, W. R., "Integrated Multidisciplinary Design Optimization of Rotorcraft," *Journal of Aircraft*, Vol. 28, No. 1, 1991, pp. 22–28.

[3]Celi, R., "Recent Applications of Design Optimization to Rotorcraft—A Survey," *Journal of Aircraft*, Vol. 36, No. 1, 1999, pp. 176–189.

[4]Celi, R., "Optimum Aeroelastic Design of Helicopter Rotors for Longitudinal Handling Qualities Improvement," *Journal of Aircraft*, Vol. 28, No. 1, 1991, pp. 49–57.

[5]Sahasrabudhe, V., and Celi, R., "Efficient Treatment of Moderate Amplitude Constraints for Handling Qualities Design Optimization," *Journal of Aircraft*, Vol. 34, No. 6, 1997, pp. 730–739.

[6]Sahasrabudhe, V., Celi, R., and Tits, A., "Integrated Rotor-Flight Control System Optimization with Aeroelastic and Handling Qualities Constraints," *Journal of Guidance, Control, and Dynamics*, Vol. 20, No. 2, 1997, pp. 217–225.

[7]Sahasrabudhe, V., and Celi, R., "Improvement of Off-Design Characteristics in Integrated Rotor-Flight Control System Optimization," *Proceedings of the 53rd Annual Forum of the American Helicopter Society*, American Helicopter Society, Alexandria, VA, 1997.

[8]"Handling Qualities Requirements for Military Rotorcraft," U.S. Army Aviation and Missile Command, Rept. ADS-33E-PRF, Redstone Arsenal, AL, March 2000.

[9]Kim, F. D., Celi, R., and Tischler, M. B., "High-Order State Space Simulation Models of Helicopter Flight Mechanics," *Journal of the American Helicopter Society*, Vol. 38, No. 2, 1993, pp. 16–27.

[10]Kim, F. D., Celi, R., and Tischler, M. B., "Forward Flight Trim Calculation and Frequency Response Validation of a High-Order Helicopter Simulation Model," *Journal of Aircraft*, Vol. 30, No. 6, 1993, pp. 854–863.

[11]Tischler, M. B., Colbourne, J. D., Morel, M. R., Biezad, D. J., Levine, W. S., and Moldoveanu, V., "CONDUIT—A New Multidisciplinary Integration Environment for Flight Control Development," NASA 112203, USAATCOM Technical Rept. 97-A-009, June 1997.

[12]Colbourne, J. D., Frost, C. R., Tischler, M. B., Cheung, K. K., Hiranaka, D. K., and Biezad, D. J., "Control Law Design and Optimization for Rotorcraft Handling Qualities Criteria Using CONDUIT," *Proceedings of the 55th Annual Forum of the American Helicopter Society*, American Helicopter Society, Alexandria, VA, 1999.

[13]Fusato, D., "Design Sensitivity Analysis and Optimization for Helicopter Handling Qualities Improvement," Ph.D. Dissertation, Dept. of Aerospace Engineering, Univ. of Maryland, College Park, MD, May 2002.

[14]Fusato, D., and Celi, R., "Design Sensitivity Analysis for Helicopter Flight Dynamic and Aeromechanical Stability," *Journal of Guidance, Control, and Dynamics*, Vol. 26, No. 6, 2003, pp. 918–927.

[15]Fusato, D., and Celi, R., "Bandwidth Sensitivity Analysis for Articulated and Hingeless Rotor Helicopters," *Journal of Guidance, Control, and Dynamics* (submitted for publication).

[16]Fusato, D., and Celi, R., "Design Sensitivity Analysis for ADS-33 Quickness Criteria and Maneuver Loads," *Proceedings of the 58th Annual Forum of the American Helicopter Society*, American Helicopter Society, Alexandria, VA, 2002.

[17]Theodore, C., and Celi, R., "Helicopter Flight Dynamic Simulation with Refined Aerodynamic and Flexible Blade Modeling," *Journal of Aircraft*, Vol. 39, No. 4, 2002, pp. 577–586.

[18]Keller, J. D., "An Investigation of Helicopter Dynamic Coupling Using an Analytical Model," *Journal of the American Helicopter Society*, Vol. 41, No. 4, 1996, pp. 322–330.

[19]Vanderplaats, G. N., *Numerical Optimization Techniques for Engineering Design: With Applications*, McGraw–Hill, New York, 1984, Chap. 6.

[20]Vanderplaats, G. N., *DOT-Design Optimization Tools, User's Manual*, VMA Engineering, Inc., Goleta, CA, May 1995.